HIGH SCHOOL EDITION
Journal of Student Research
Volume 10 Issue 3 (2021)

A Novel Thermoplasmonic Paint with Titanium Nitride Nanoparticles

Rhiaan Jhaveri[1] and Ravi Mariwala[#]

[1]Dhirubhai Ambani International School, Bandra (East), Mumbai, India
[#]Advisor

ABSTRACT

Several studies have reported the photothermal heating of colloidal nanoparticles due to plasmon-enhanced light absorption, and Titanium Nitride has emerged as a promising nanomaterial for the practical application of this phenomenon. Here, we developed a novel paint that is infused with Titanium Nitride nanoparticles. Varying concentrations of this paint were applied to copper plates and tested under natural light. Substantial heating was observed under both high-grade and low-grade light for the higher concentrations. The uses of this source of heat extend to long-term solutions for reducing the prevalence of waterborne diseases in remote, rural settings via pasteurization.

Introduction

Interaction of light with metal nanoparticles / Thermoplasmonics

The novel field of thermoplasmonics has been a growing interest in recent years due to its wide range of applications, including in drug delivery, cancer treatment, and photovoltaic cells. There have also been breakthroughs by companies such as Syzygy Plasmonics in the photocatalysis of chemical reactions, driven by hot-carriers [1]. The underlying principle consists of photoexcitation, which is the wavelength-dependent absorption of light by an electron. [2]
Due to the existence of discrete quantized energy levels, photons may be absorbed when they possess energy equal to the energy between the ground and excited state of an electron, leading to the excitation of an electron (or conversely, a photon may be emitted and an excited species may go to a lower energy level). Generally, the energy of a photon is governed by the well-known equations:

$$E = h\nu$$

$$\nu = \frac{c}{\lambda}$$

However, because the transition of electrons can be combined with vibrational transitions, materials generally can absorb continuous spectra of wavelengths.

This interaction, however, changes at the nanoscale. All photons incident on a nanoparticle (NP) are either scattered or absorbed. When NPs of certain sizes, shapes and material are struck by electromagnetic radiation of a frequency which matches the natural frequency at which their surface electrons oscillate, they exhibit local surface plasmon resonance (LSPR). In these NPs, for example gold, LSPR allows for a much higher light absorption cross-section than is usually possible. Additionally, at the nanoscale, the work function of metals increases, due to which electrons can be excited to a broader range of energy levels without escaping confinement. Thus, electrons relax to

lower energy levels, electron-electron heat transfer occurs, and heat is eventually transferred by conduction to the surrounding medium. This phenomenon of plasmon-enhanced light absorption and subsequent local heating has developed into one of the major sub-fields in plasmonics, termed as plasmonic heating or 'thermoplasmonics' [3].
Generally, for spherical thermoplasmonic NPs in a uniform surrounding medium, the actual temperature increase is given by:

$$T_{NP} = \frac{\sigma_{abs} I}{4\pi \cdot k_s a}$$

Where a is the radius of a single spherical NP, σ_{abs} is the absorption cross-section (proportional to volume), I is the light intensity (power per unit area), and k_s is the thermal conductivity of the surrounding medium.

Optimisation for Solar Energy

When considering the most favourable metal nanoparticles for use in solar energy conversion, a number of species have been proven to be better than others. These involve single-walled carbon nanotubes (SWCNTs) [4], Gold nanospheres [5], and tungsten nitride [6]. More recently, Titanium Nitride (TiN) has emerged as an alternative to metal nanoparticles. Gold NPs are well-known to support localized surface plasmon resonances (LSPRs), which enhance both scattering and absorption. However, TiN NPs are of particular interest due to their relatively easy availability for commercial applications and their stability under high temperatures and extended periods of time, which prevents them from photo-bleaching, unlike other NPs. More significantly, TiN NPs exhibit a broad absorption spectrum with a peak in the visible and near-infrared (NIR) range, which coincides with the peak of the solar emission spectrum [7]. The absorption cross-section for TiN NPs of 50 nm has been experimentally determined to be near-unity for light of wavelengths around 750 nm [8]. At its maximum, the sun's intensity is around $1380\ W \cdot m^{-1}K^{-1}$. A thin coating of enamel paint has a thermal conductivity of $0.2\ W \cdot m^{-1}K^{-1}$. Thus, increase in local temperature for a single TiN NP can be calculated using the aforementioned formula:

$$T_{NP} = \frac{1 \cdot 1380}{4\pi \cdot 0.2 \cdot 50} = 11.0℃$$

Absorption Efficiencies

The superior absorption of sunlight by TiN can be confirmed by its performance in the colloidal form, in which it has an integrated absorption efficiency of approximately double that of gold or carbon NPs and shows a 2-4 times higher rate of temperature increase than carbon NPs [9].

In the present work, we seek to formulate a new type of paint that contains TiN nanopowder for use in solar-absorbing applications and to facilitate the enhanced heating of a metal substrate. This paint would contain colloidal TiN and hence retain its LSPR-related properties, and would be black to retain absorption of sunlight in the visible and NIR regions. It would be preferable to have maximum TiN NPs on the surface, to be exposed to sunlight.

Materials and Methods

TiN nanopowder of average particle size 40-50 nm was selected for the preparation of the paint. The nanopowder was purchased directly from a manufacturer and was synthesized by co-precipitation, with purity 99.9%. Different masses of NPs (0.2g, 0.5g and 1g) were evenly dispersed in 2ml of turpentine to prevent coagulation and clumping. This was then mixed in 8ml of industrial-grade black enamel paint which was used to double-coat $5cm \times 5cm$ copper plates.

One copper plate was coated in black paint without TiN NPs to serve as the control. The resultant mixtures were thus of concentrations (g/ml expressed as % v/w): 2%, 5%, 10% and 0% (control).

The coated plates were placed in natural sunlight. Temperature was measured using Type-K surface thermocouple probes which were adhesive and were stuck to the bottom surface of the copper plates. Excluding the top, painted portion, the rest of the plate was surrounded in glass wool (with thickness ~3 inches) for thermal insulation. Wind was kept out using a plastic draught shield.

The experiment was carried out in two types of lighting conditions: low-grade light of ~40,000 lux (7:00 - 9:15 AM) and high-grade light of ~80,000 lux (10:20 -11:50 AM). To see the full effect of low-grade light, the time was extended.

Results and Analysis

The four different measured temperatures were averaged across 3 trials for each concentration of TiN NPs in paint. These mean concentrations were plotted against time, once for high-grade light and once for low-grade. The maximum temperatures reached were also plotted against concentration. Lastly, the temperature changes relative to the control (in %) was plotted as a function of time.

High-grade light

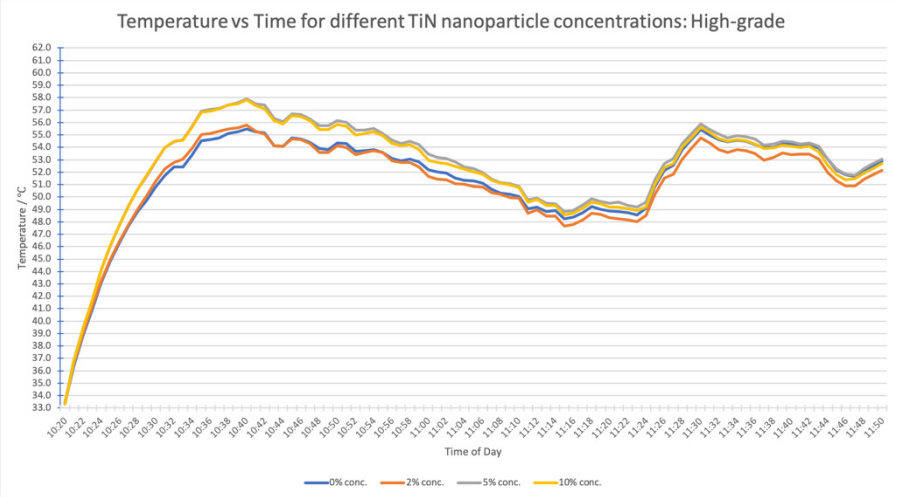

Fig. 1. Temperature vs time for different concentrations of Titanium Nitride nanoparticles under high-grade light

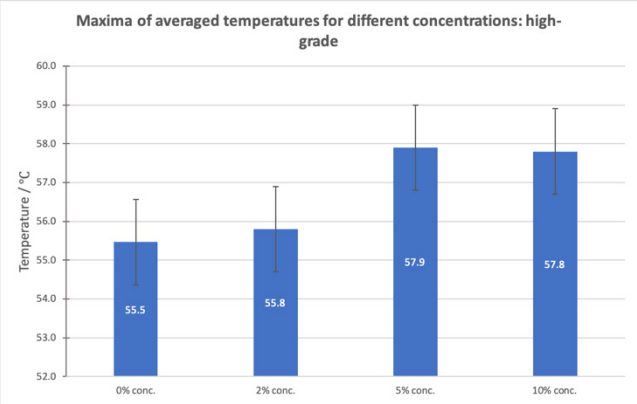

Fig. 2. Maxima of averaged temperatures for different concentrations under high-grade light

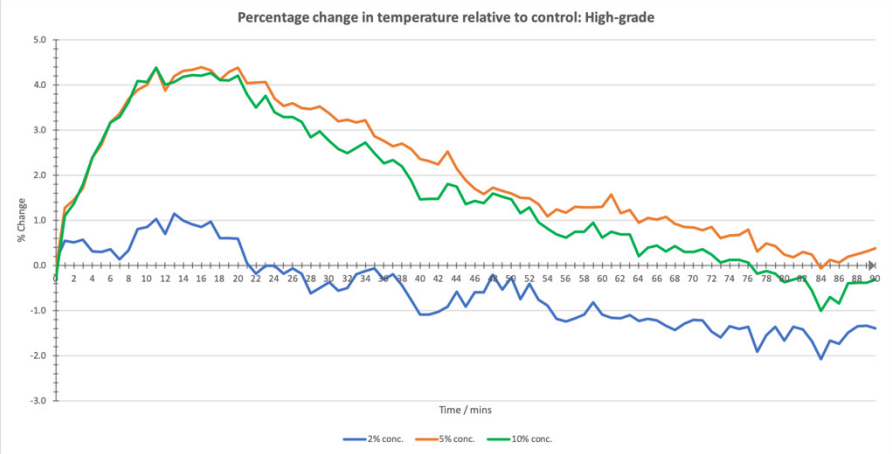

Fig. 3. Percentage change in temperature relative to control under high-grade light

As can be seen in Figure 1, when left under high-grade sunlight, all 4 concentrations undergo, at first, a steep rise in temperature. For around the first 4 minutes, the 4 concentrations each have almost a constant rate of temperature increase of 10.8 ℃/sec. This rate undergoes a gradual decrease across the 4 concentrations, and around 43 ℃, a distinct separation is seen between the graphs of the 0 and 2 % w.v. concentrations and the 5 and 10 % w.v. concentrations. The separation becomes gradually more pronounced, and is at its maximum when there is a difference of ~2.5℃ at around 10:38, - just minutes away from the overall peak time of each of the 4 concentrations. At 10:40 (20 minutes in), all four concentrations reach their maximums. This is depicted in Figure 2 - we can see that the maxima for the 10% and 5% concentrations are nearly the same: 57.8 and 57.9 ℃ respectively, whereas for 2% and 0%, they are 55.8 and 55.5℃.

After the peak, this trend nearly reverses - the separation decreases till the 4 concentrations almost merge; this is also observed in Figure 3, where the % change relative to the control after 65 minutes (11:25) is <1% Although a ‘secondary peak’ is reached at 11:30 in Figure 1, this can be disregarded due to the information in Figure 3, from which we can deduce that this peak is probably due to ambient temperature changes and not plasmonic heating. The

only 'true' peak that we can attribute to plasmonic heating is the primary one (10:40), since it is here that we observe the highest relative increases of >4%.

Moreover, we can confirm the presence of some thermoplasmonic heating in the 5% and 10% plates by studying the slopes of their graphs in Figure 3. After the peak, the slopes of all three graphs are roughly the same in magnitude, and negative - this indicates consistent loss of heat over an extended period of time, till the temperature of the control is reached. Thus, we see the presence of excess heat in these two plates, formed rapidly within the first 20 minutes and eventually lost to the surroundings, and this could be due to the gradual dissipation of localised heat from the NPs.

It is also important to note that the 2% concentration is consistently lower than the other temperatures from 10:46 to the end of the experiment. The difference is more anomalous towards the end, however, when three of the other concentrations, including the control, merge into a single temperature while the 2% concentration is about a degree lower. This could be attributed to some sort of systematic error with the insulation.

Low-grade light

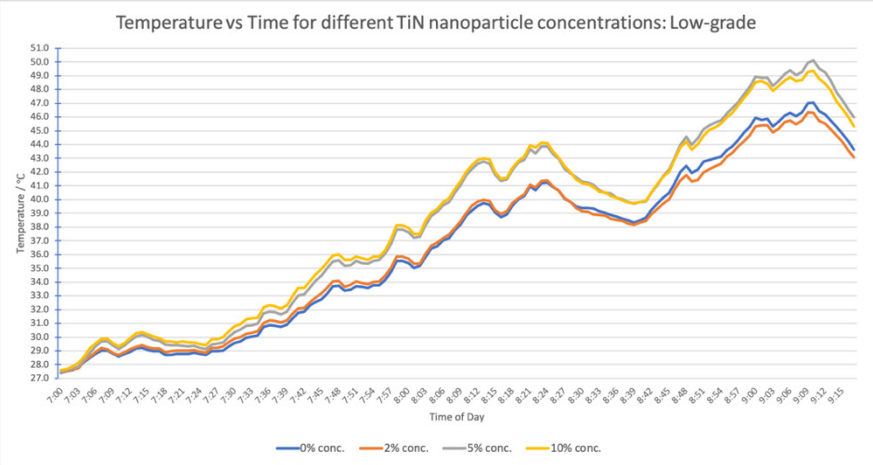

Fig. 4. Temperature vs time for different concentrations of Titanium Nitride nanoparticles under low-grade light

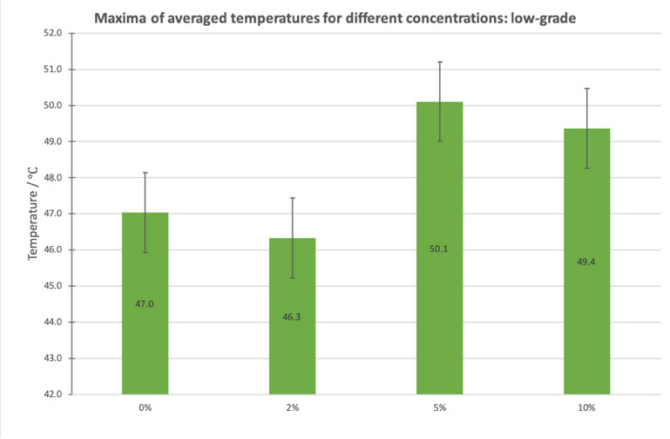

Fig. 5. Maxima of averaged temperatures for different concentrations under low-grade light

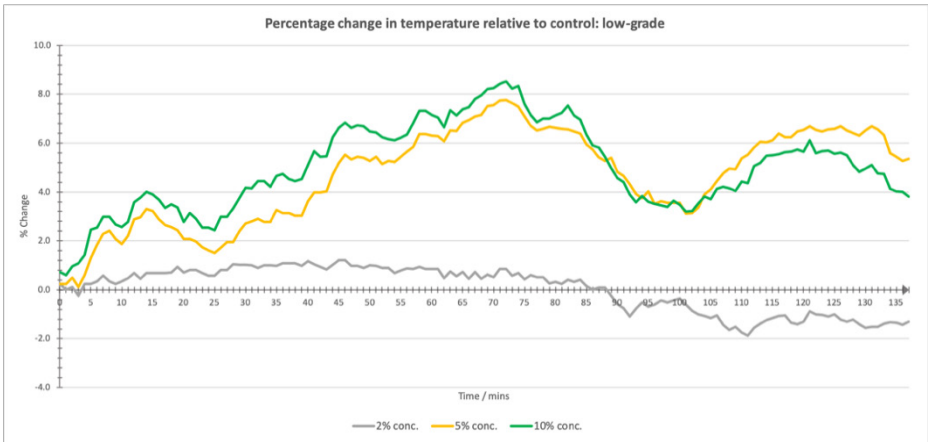

Fig. 6. Percentage change in temperature relative to control under low-grade light

Investigating the same concentrations of paint under low-grade light yields both similarities and differences in observations.

Like in high-grade light, a distinct separation is seen between the graphs of the 0 and 2 % w.v. concentrations and the 5 and 10 % w.v. concentrations in Figure 4. However, this separation begins just 3 minutes in, becomes gradually more pronounced, and is consistent till the end. The separation is at its maximum when there is a difference of ~3.5℃ at 9:09. Additionally, the slope of each graph in Figure 4 - and hence the rate of temperature increase - is lower than the initial slopes in Figure 1, which is expected from low-grade light.

We can observe a primary peak at 9:10/130 minutes, a secondary peak at 8:24/84 minutes, and many more sub-peaks. Once again, the 2% concentration is partially anomalous, because as seen in Figure 6, there is a negative change relative to the control - yet, this does not affect the distinct difference between the maxima of 0%, 2% and 5%, 10%, which are well outside the limits of experimental error in Figure 5.

Hence for low-grade light, we note more gradual, sustained heating over a larger period of time (135 minutes). This is confirmed in Figure 6, which depicts the 5% and 10% concentrations as consistently higher than the control, and amongst themselves some crossing and variance that can be attributed, with certainty, to fluctuations in ambient temperature and/or lighting, since the trend is followed by each graph. When considering the slope of graphs in Figure 6, we see that low-grade light produces temperatures that gradually increase, but rarely dissipate, unlike for high-grade light in which the peak was followed by a steady emission of radiation. This could be because low-grade light enables the NPs to release localised heat incrementally.

Discussion and Conclusion

From the quantitative analysis, it is evident that the thermoplasmonic effect exists under both high-grade and low-grade light: for low-grade light, sustained periods of time result in gradual heating. Additionally, the 2% concentration paint displayed almost no heating relative to the control - this could be because the quantity of TiN nanopowder, 0.2g, was not sufficient enough to be even partially exposed to the surface of the metal substrate. This could be eliminated with not only higher concentrations of the nanopowder in paint, but also methods such as laboratory spin-coating to cover the substrate (albeit unsuitable for practical, large-scale applications of paint), or the sonication of the colloidal NPs to ensure an even spread of them on the substrate, in order to maximise their surface area.

Nevertheless, the formulation of a 'thermoplasmonic paint' with significant photo-thermal properties has been shown. This type of paint exhibits a heating time of approximately 2 hours to reach a maximum; thus, its applications may be especially seen in the usage of low-grade thermal energy by conductive surfaces (since the present investigation uses a coated metal substrate as a transducer of heat.

A thermoplasmonic paint-enabled solar cell could be used in spacecraft and space exploration vehicles. This energy source seems to be a suitable substitute for radioisotope thermoelectric generators (RTGs), which were used in the NASA Voyager probes [10], and have also been included in realistic proposals for interstellar probes by NASA [11]. These are nuclear batteries used in low-maintenance, low-power situations for durations too long and impractical for traditional fuel cells or solar cells. The stability over time, as well as resistance to photo-decay of TiN is an added benefit to such an energy source. Thermoplasmonic paint will also eliminate the safety hazards associated with the radioactive materials in RTGs, and hence is a lucrative alternative [12].

Terrestrially, too, thermoplasmonic paint is a possible substitute for some solar applications. As the experiment has shown, especially in the case of low-grade light, due to the continuously high relative temperature and its incremental release to the surroundings, TiN NPs may be useful in the immediate storage and release of thermal energy to the surroundings, which is a feature that photovoltaics falls short in, as there is an inevitable loss of thermal energy when energy is converted from one form to another and back (solar energy converts light energy to electric and subsequently chemical energy, and reverts this when energy is required to be drawn from batteries). Thermoplasmonic paint eliminates this and offers a direct photo-thermal effect, bypassing peripheral losses of energy. However, one shortcoming (in the paint as well as in the general domain of thermoplasmonics) is that the energy cannot be drawn and utilized in a controlled, deliberate manner yet.

With the above-mentioned characteristics of the thermoplasmonic paint in mind, another realistic application may be in the process of pasteurisation and water disinfection. Pasteurisation of water occurs when its temperature is raised to 65 ℃ for 3 minutes [13]. As evidenced by the experiment, the thermoplasmonic paint can sustain heating for periods much larger than 3 minutes, and is capable of reaching temperatures ~60 ℃ with a 5-10% concentration; thus, it is hypothesised that at slightly higher concentrations, solar disinfection (SODIS) would be possible. Also, one process of pasteurising fluids such as water involves the passing of water through 'plate heat-exchangers', which are essentially thin metal plates with temperatures of low magnitudes [14]. This is almost exactly replicable by the current experimental setup, wherein thin metal plates have been used, and this could result in a significant carbon reduction from existing energy-intensive heat-exchanger systems.

Thus, theoretically, clean water can be produced at a near-continuous rate after prior heating of the plates to the optimum temperature, which would be extremely beneficial to rural areas and villages with lack of access to safe potable water and who receive sufficient sunlight, because while pasteurisation does not sterilise water, it reduces the number of pathogens by many orders of magnitude and hence can reduce the incidence of water-borne diseases by 35-40% [15]. Since this method works in low-grade light, water disinfection could be available to the people from ~07:00 to evening-time. The low maintenance associated with thermoplasmonic paint, in addition to the other advantages, makes this a seemingly sustainable and long-term solution.

Acknowledgements

The author would like to acknowledge Dr. Ravi Mariwala for his guidance throughout the process of research.

References

[1] Robatjazi, H., Bao, J. L., Zhang, M., Zhou, L., Christopher, P., Carter, E. A., . . . Halas, N. J. (2020). Plasmon-driven carbon–fluorine (C(sp3)–F) bond activation with mechanistic insights into hot-carrier-mediated pathways. Nature Catalysis, 3(7), 564-573. doi:10.1038/s41929-020-0466-5

[2] Baffou, G., Cichos, F., & Quidant, R. (2020). Applications and challenges of thermoplasmonics. Nature Materials, 19(9), 946-958. doi:10.1038/s41563-020-0740-6

[3] Maier, S. A. (2017). World Scientific Handbook of Metamaterials and Plasmonics. World Scientific Handbook of Metamaterials and Plasmonics. doi:10.1142/10642-vol1

[4] Tune, D. D., & Shapter, J. G. (2013). The potential sunlight harvesting efficiency of carbon nanotube solar cells. Energy & Environmental Science, 6(9), 2572. doi:10.1039/c3ee41731j

[5] Neumann, O., Urban, A. S., Day, J., Lal, S., Nordlander, P., & Halas, N. J. (2012). Solar Vapor Generation Enabled by Nanoparticles. ACS Nano, 7(1), 42-49. doi:10.1021/nn304948h

[6] Zhang, C., Wang, S., Chen, Z., Fan, J., Zhong, Z., & Zhang, X. (2019). A tungsten nitride-based degradable nanoplatform for dual-modal image-guided combinatorial chemo-photothermal therapy of tumors. Nanoscale, 11(4), 2027-2036. doi:10.1039/c8nr09064e

[7] Ishii, S., Sugavaneshwar, R. P., & Nagao, T. (2016). Titanium Nitride Nanoparticles as Plasmonic Solar Heat Transducers. The Journal of Physical Chemistry C, 120(4), 2343-2348. doi:10.1021/acs.jpcc.5b09604

[8] Guler, U., Suslov, S., Kildishev, A. V., Boltasseva, A., & Shalaev, V. M. (2015). Colloidal Plasmonic Titanium Nitride Nanoparticles: Properties and Applications. Nanophotonics, 4(3), 269-276. doi:10.1515/nanoph-2015-0017

[9] Ishii, S., Sugavaneshwar, R. P., Chen, K., Dao, T. D., & Nagao, T. (2015). Sunlight absorbing titanium nitride nanoparticles. 2015 17th International Conference on Transparent Optical Networks (ICTON). doi:10.1109/icton.2015.7193490

[10] Voyager - Spacecraft - Radioisotope Thermoelectric Generators (RTG). (n.d.). Retrieved from https://voyager.jpl.nasa.gov/mission/spacecraft/instruments/rtg/

[11] Innovative Interstellar Probe. (n.d.). Retrieved from http://interstellarexplorer.jhuapl.edu/index.php

[12] Jaziri, N., Boughamoura, A., Müller, J., Mezghani, B., Tounsi, F., & Ismail, M. (2020). A comprehensive review of Thermoelectric Generators: Technologies and common applications. Energy Reports, 6, 264-287. doi:10.1016/j.egyr.2019.12.011

[13] Islam, M. F., & Johnston, R. B. (2006). Household pasteurization of drinking-water: the chulli water-treatment system. Journal of health, population, and nutrition, 24(3), 356–362.

[14] Vieira, M., Pereira, J., & Lucher, C. (2008). Pasteurization with a Plate Heat Exchanger. Experiments in Unit Operations and Processing of Foods, 113-123. doi:10.1007/978-0-387-68642-4_15

[15] Fewtrell, L., Kaufmann, R. B., Kay, D., Enanoria, W., Haller, L., & Colford, J. M. (2005). Water, sanitation, and hygiene interventions to reduce diarrhoea in less developed countries: A systematic review and meta-analysis. The Lancet Infectious Diseases, 5(1), 42-52. doi:10.1016/s1473-3099(04)01253-8